Design criteria and performance analysis of a smart portable device for leak detection in water transmission mains

B. Brunone[1], C. Capponi, and S. Meniconi
Department of Civil and Environmental Engineering, The University of Perugia

via G. Duranti 93, 06125 Perugia, Italy

Abstract

In this paper, criteria for the optimal and market-oriented design of the Smart-Portable Pressure Wave Maker (S-PPWM) device are presented. The outlined criteria are based on the positive results obtained both in laboratory and real systems. The S-PPWM can be used for fault (e.g., leak) detection in pressurized transmission mains (TMs) within the so-called Transient Test-Based Techniques. The proposed design procedure addresses two crucial issues: i) to minimize the volume (and then improving the portability), and ii) to allow evaluating easily the minimum detectable leak, for a given test TM. Such a procedure takes into account the characteristics and functioning conditions of the test TM. In such a context, the safety of the test TM in terms of maximum generated overpressures and air entry prevention during transient tests is taken into account.

1. Introduction

Pressurised transmission mains (TMs) are important infrastructures conveying water from the source to a distribution network (WDN). Thus, the consequences of a TM failure are more severe than for a distribution main. However, best practices for water loss management (e.g.,[1]) are mainly focused on WDNs on the unjustified assumption that TMs rarely leak. On the

[1]corresponding author, e-mail: bruno.brunone@unipg.it

contrary, recent worldwide surveys on large diameter TMs show that their actual leakage is much larger than expected [2, 3]. Such a feature makes leak detection in TMs a key component of water loss control programs for improving the efficiency of water systems. In fact, the rehabilitation and/or replacement of aging and deteriorated TMs need to be considered as close as to the end of their useful life since such interventions are more expensive than for WDNs. These are the reasons of the growing awareness in the water industry and research centers about the development of new technologies for fault (e.g., leak) detection in TMs. Even if a benchmark analysis of the available techniques is beyond the aims of this paper, a concise description of the most widespread ones seems important in order to place the proposed device in context. Moreover, it is worth of noting that a benchmark analysis would not be an easy task since most of methods are based on technologies covered by industrial secrecy and not well documented in scientific papers.

With specific reference to leak detection in TMs, the available techniques take inspiration from very different principles. A possible classification can be based on the degree of interference with the test pipe. Such an approach is justified by the larger laying depth in TMs with respect to WDNs. Such a feature has two consequences. The first is that any intervention is more expensive in TMs because of not only the excavation cost but also the longer duration. The second consequence is that some viable techniques cannot be used; the ground penetrating radar, as an example, can explore the ground to a depth of up to 200 cm [4]. As a consequence, the use of this or that technique may depend on the relevance of the interventions to execute before it can be operational or, in a word, on the invasiveness of the technique. According to such an approach, invasive techniques can be defined those requiring inserting probes or installing devices along the pipe route. On the contrary, non-invasive techniques are those where measurements are at a distance or executed at the very few existing access points.

The family of invasive techniques includes acoustic methods – e.g., the SmartBall and Sahara inspection platforms, by PureTechnologies-Xylem Inc., the EchoShore-TX platform, by Echologics-Mueller Water Products [4, 1] – and the electromagnetic ones [5, 6]. The SmartBall inspection platform consists in a free-swimming inspection ball, equipped with a highly sensitive acoustic sensor, travelling with the water flow recording the acoustic environment within the line. Two 100 mm access points are needed: one for insertion and another for extraction of the device; the data is stored on the device and analyzed upon completion of the inspection. On the contrary, the

Sahara inspection platform uses a tethered inspection tool and then only one access point is needed. For both SmartBall and Sahara platforms, the length of the pipeline that can be inspected is not explicitly indicated but it should be of the order of some kilometres (details about some case studies can be found at puretechltd.com/case-studies). At the heart of the EchoShore-TX platform is a node – equipped with acoustic sensors – which consists also of a data processor, communication hardware and a battery power source. Nodes are typically installed in an access chamber along the desired length of the TM to be monitored; monitoring zones extend up to some kilometres. It is worth of noting that it may be quite hard to interpret acoustic signals due to, as an example, signal similarities. As a consequence, to improve the performance of the acoustic methods, the use of the wavelet transform [7] and advanced algorithm for the analysis of the measured data have been proposed [8]. When methods based on the propagation of electromagnetic waves are used, a wire-like sensing element must be buried along the test pipe [5, 6]. This makes this technique very invasive as it implies a relevant excavation. As a consequence, such a method is usable mostly for new pipes or rehabilitated branches.

The family of the non-invasive methods counts on data from satellite-based and transient test-based (TTBTs) techniques. Data from satellite driven techniques (e.g., utiliscorp.com) use satellite images that cover large areas (each image covers approximately 3,500 km^2, depending on satellite). Such techniques are based on the fact that L-rays sent to the earth are able to penetrate into the soil and register the existence of traces of drinking water, leaked from the water systems. Accordingly, such techniques require no capital investment or device installation (more details about the method and some case studies can be found at puretechltd.com/case-studies). It is worth of noting that the performance of such techniques improves when the "density" of pipes is large (i.e., they perform better for WDNs). TTBTs are non-invasive techniques originating from the well-known dynamics of transients in a pressurized flow [9, 10]. The necessary premise to the TTBTs is the generation of a transient with the insertion of a controlled pressure wave, Δ, into the test pipe. Successively, such a pressure wave explores the pipe travelling away from the place where it was generated with a velocity equal to the pressure wave speed, a. If the pressure wave encounters a discontinuity or a defect (e.g., a leak), a smaller size pressure wave, Δ_R, is reflected back towards where it came. At the same time, a transmitted wave, Δ_T, proceeds forward continuing the exploration of the downstream part of the test pipe

[11]. During the successive phases of the test, the transient response exhibits a more important damping of the pressure peaks with respect to the defect-free pipe [12]. In brief, the reflected and transmitted pressure waves and larger damping represent a sort of fingerprints of the discontinuities/defects in the pressure time-history (hereafter referred to as *pressure signal*, h). It is important to note that the size and characteristics of such fingerprints depend on the ones of the discontinuity/defects. In the case of a leak, as an example, the larger the leak, the larger both the negative pressure wave reflected back and the induced damping of the pressure peaks. As a consequence, capturing the signal at a suitable measurement section in the TM can provide useful information about its state. A discussion about the possible approaches for analysing effectively the pressure signals measured during transient tests is reported in some review papers (e.g., [13, 14, 15, 16, 17]).

This paper is focused on TTBTs with particular regard to the generation of appropriate transient tests. The term appropriate has two implications on the characteristics of the inserted pressure wave, Δ. The first concerns its size that must be small – i.e., few meters of water column – to not damage the test pipe. Such a shrewdness in terms of transient severity drastically reduces the risk of pipe failure due to transient tests. The second implication is about its sharpness – the sharper the better [18] – that implies the execution of fast maneuvers (i.e., with a duration of few dozens of milliseconds, as an order of magnitude). To address such requirements, some devices have been proposed based on the two possible ways to generate a pressure wave: by a sudden change of the mean velocity or pressure head. In the first case, a valve is closed or a pump is switched-off. In [19] a valve is installed on the top of a standpipe connected to a fire hydrant. Such a device allows controlling the generated pressure wave by fixing an adequate value of the discharge through the valve in the pre-transient conditions. A further option is the device described in [20, 21], where a length of a small diameter copper pipe, with a solenoid valve at the top, is fitted to a fire hydrant cap. The fast closure of such a valve creates two small pressure waves travelling up and downstream through the pipe. When the transient is caused by a pump switch-off, an appropriate precaution is to reduce the pre-transient discharge to control the generated overpressure. More focused on the industrial field are the devices proposed in [22, 23] to investigate the dynamics of hydraulic components with a short response time. A sudden change of the pressure head can be generated by connecting a device where the pressure is larger than the one in the test pipe. This is the case of the Portable Pressure

Wave Maker (PPWM) device. As a further option – until now used only for laboratory tests – Gong et al. [24] suggest a transient wave generator which uses controlled electrical sparks.

As a general comment, it is worth of noting that none of the above techniques for generating Δ may be preferred over the others in any test pipe. In fact, in most cases, the choice of the method to use strongly depends on the characteristics of the test pipe and its functioning conditions. Rather, good results may be achieved by associating different techniques (e.g., [25]).

This paper is focused on the Smart-Portable Pressure Wave Maker (S-PPWM) device, an optimized version of the PPWM one (S as smart). Precisely, following the encouraging results of the tests executed both in laboratory ([26, 18, 27, 28]) and real systems ([25]) with different characteristics (i.e., both in metallic and polymeric pipe systems), viable design criteria of the S-PPWM are needed to enable the use of such a device in an ever-widening range of TMs. Accordingly, this paper is organized as follows. In the next section, as a necessary premise, the layout and behavior of the S-PPWM device are briefly illustrated. Then, the mentioned novelty of this paper is offered: the identification of rational design criteria of the device and the procedures for its successive performance assessment and design refinement. Then, the related operative design procedure is synthesized in a flowchart graph where the needed preliminary measurements, input data, model results, decisions, and output are clearly highlighted. Finally, the key results from this study are highlighted in the Conclusions.

2. The Smart-Portable Pressure Wave Maker (S-PPWM)

The Smart-Portable Pressure Wave Maker (S-PPWM) (Fig.1) has been refined at the Water Engineering Laboratory (WEL) of the University of Perugia, Italy. It consists of a steel vessel, filled with water and air, which can be pressurised by means of a standard air compressor. The S-PPWM and test pipe are linked by a short conduit with a small-diameter connection valve (CV) at its end. The behavior of the S-PPWM is illustrated in Fig. 2 when, as an example, it is installed in a single pipe. Such a pipe, with a constant internal diameter, D, and length L, is supplied by a reservoir, R, with a constant level, h^R. A leak is placed at a distance x^l from the downstream end section (hereafter, x indicates the axial co-ordinate, and superscript l refers quantities to the leak).

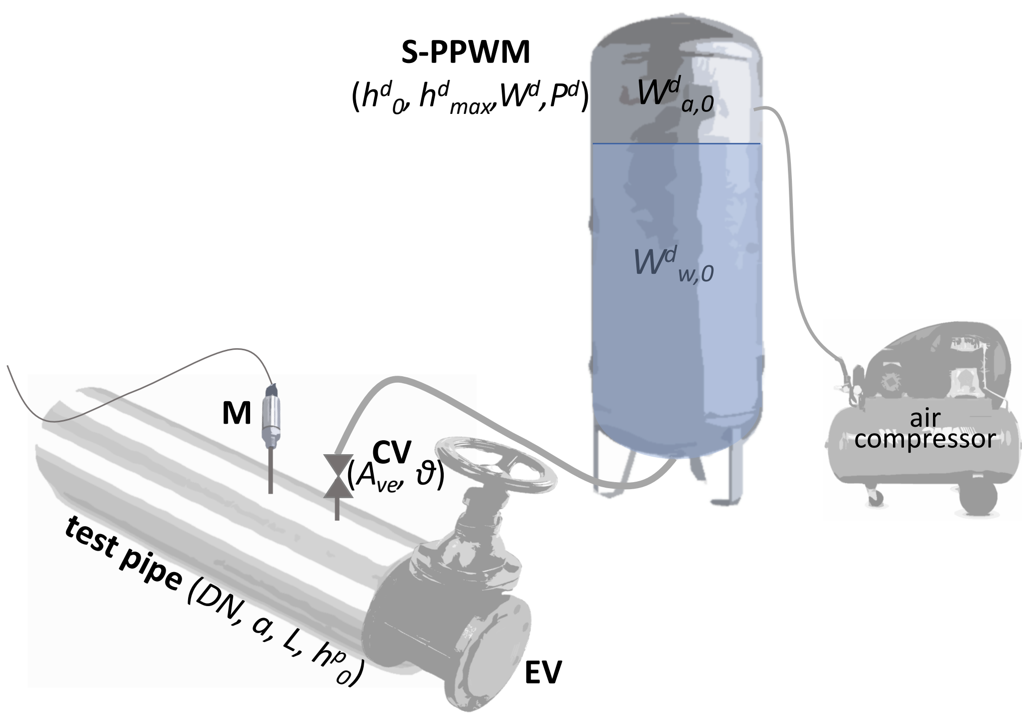

Figure 1: The Smart-Portable Pressure Wave Maker (S-PPWM) device, its installation at the downstream section of a TM with the end valve (EV) fully closed, and quantities characterizing the pipe (nominal diameter DN; pressure wave speed, a; length, L; pre-transient pressure head, h_0^p); the S-PPWM device (pre-transient pressure head, h_0^d; maximum allowable pressure head, h_{max}^d; total volume, W^d; total weight, P^d; pre-transient water volume, $W_{w,0}^d$; pre-transient air volume, $W_{w,0}^d$); and the connection valve CV (effective area, A_{ve}; duration of the opening maneuver, θ).

In a possible arrangement of the survey for leak detection, the S-PPWM is placed at the downstream end section of the leaky pipe with the end valve EV fully closed. Because of the poor accessibility of TMs, usually the pressure signal is acquired at section M, immediately upstream of the S-PPWM. Before starting the survey, the pressure head inside the S-PPWM is set at a value, h_0^d, larger than the one in the pipe, h_0^p (the superscripts d and p refer quantities to the S-PPWM device and test pipe, respectively, and the subscript 0 indicates the pre-transient conditions). The successive opening of the CV generates a pressure wave, Δ, propagating into the pipe (phase I in Fig. 2). The entity of the pressure wave generated by the S-PPWM can be fixed precisely by adjusting the difference h_0^d - h_0^p. It is worth noting that, because of its small size, the CV can be opened very quickly and then it generates a sharp pressure wave. At time $t = x^l/a$ (phase II), the interaction of Δ with the leak gives rise to a (negative) reflected, Δ_R, and (positive) transmitted, Δ_T, pressure wave [9]. Then, the reflected wave travels back toward the downstream end section. At time $t = 2x^l/a$, it doubles at section M since the EV is fully closed (phase III). It is important to note that actually the size of the pressure wave decreases while travelling along the pipe. This is due to friction and interaction with pipe material (for polymeric pipes). As a consequence, the pressure wave interacting with the leak is smaller than Δ as well as the one reaching section M is smaller than Δ_R. However, during phases II and III such differences can be neglected [29]. In fact, most of the pressure decay happens after the first pipe characteristic time, τ $(= 2L/a)$.

3. Transient behavior of the S-PPWM

As mentioned, the most distinctive feature of the S-PPWM – successfully tested both in the laboratory [30, 27, 18, 28] and in real systems [25] – is to generate a pressure wave of a specified size, Δ. Such a quantity measures its potential in terms of the smallest detectable leak. In fact, for a given leak, the larger Δ, the larger Δ_R, the more reliable its identification in the measured pressure signal. However, to maximize Δ cannot be assumed as the only design criterion.

3.1. Quantities affecting the generated pressure wave

As shown in [26], the instantaneous (in practise, very fast) opening maneuver of the CV generates a pressure wave with a size, Δ, given by the following relationship:

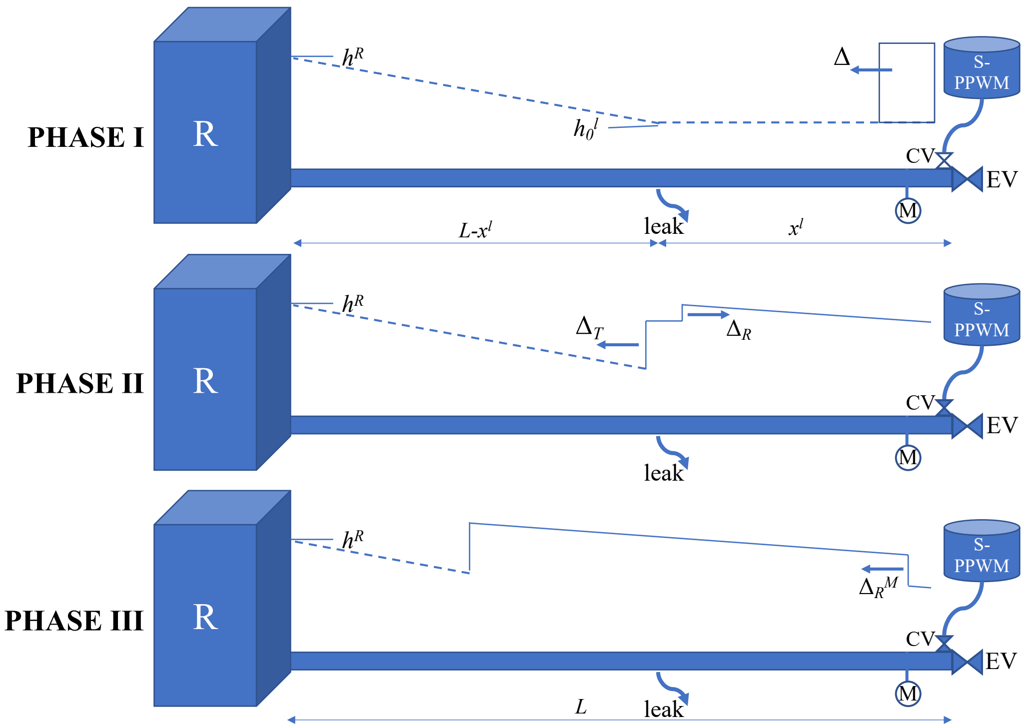

Figure 2: Transient behavior of a single leaky pipe when connected to the Smart-Portable Pressure Wave Maker (S-PPWM). The three highlighted phases concern the generation of the pressure wave, Δ (phase I), its interaction with the leak (phase II), and the interaction of the wave reflected by the leak, Δ_R, with the fully closed end valve EV at the measurement section M (phase III).

$$\Delta = \frac{1}{g}\left(\frac{aA_{ve}}{A}\right)^2\left[\sqrt{1+\frac{2g(h_0^d-h_0^p)}{\left(\frac{aA_{ve}}{A}\right)^2}}-1\right] \tag{1}$$

where g = acceleration of gravity, A_{ve} = effective area of the CV (fully open), and A = test pipe cross-sectional area.
According to Eq. (1), quantities affecting Δ, are highlighted in the following functional relationship:

$$\Delta = f_1\left[a, A, h_0^d, h_0^p, A_{ve}\right] \tag{2}$$

that indicates clearly that the value of Δ is the result of a combination of factors: the characteristics of the test pipe and CV, and pre-transient pressure regime. For a given Δ, the sharper the pressure wave reflected by the leak the more its detectability. Such a feature depends mainly on the duration, θ, of the CV opening maneuver. Precisely, the smaller θ the sharper the pressure wave. Then in the below analysis, only fast maneuvers will be considered for which $\theta \ll \tau$.
Putting aside the characteristics of the test pipe (i.e., a and A) that cannot be changed, the choice of suitable values of h_0^d, h_0^p, and A_{ve} merits some preliminary comments on the basis of Eq. (1).
For given h_0^d and A_{ve}, the smaller h_0^p, the larger Δ. Moreover, according to [31] and [32], for given leak and Δ, the smaller the pre-transient pressure at the leak, h_0^l (Fig. 2), the larger Δ_R. As a result, it is suitable to execute transient tests with the minimum value of h_0^p, and then h_0^l, compatible with the characteristics of the test pipe. However, it must be noted that it may be quite hard to decrease noticeably the pressure regime in the test pipe since it depends on the value at the supply head, h^R.
For given h_0^p and A_{ve}, the larger h_0^d, the larger Δ. However, an obvious limitation to the value of h_0^d derives from the corresponding needed mechanical strength of the S-PPWM wall. Precisely, for given material and volume, W^d, the larger h_0^d, the larger the thickness of the device and then its weight, P^d. As a consequence, in terms of the S-PPWM portability, for a given volume, it is important to minimize P^d and then h_0^d. As shown in Fig. 3, for both the considered values of W^d, P^d increases rapidly with the maximum admissible value of the internal pressure head, h_{max}^d. It is important pointing out that, in the below analysis, it is assumed $h_0^d = h_{max}^d$. A further constraint for h_0^d derives from legislation governing the use of high-pressure vessels. Precisely,

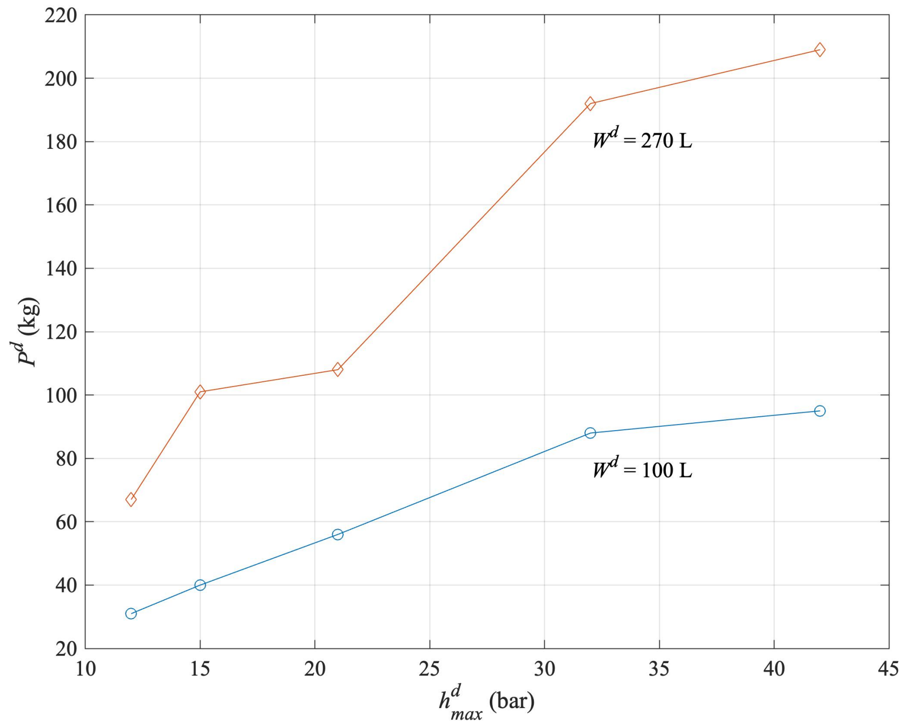

Figure 3: S-PPWM device weight, P^d, vs. the maximum maximum allowable pressure head, h^d_{max}, for two values of the total volume, W^d *[source: Baglioni stainless steel vessel catalogue, Perugia, Italy]*

when h^d_{max} is larger than a critical value, h_{crit}, more severe rules are prescribed in terms, as an example, of safety in the workplace. Moreover, to generate a large value of h^d_0, a high-power air compressor is required. Such an aspect must be taken into account when field tests are executed and the energy supply must be guaranteed by a portable AC generator.

With regard to the role of the characteristics of the CV, the larger A_{ve}, the larger Δ. However, the larger A_{ve}, the larger the duration of the opening maneuver, θ, and then the less sharp the generated pressure wave. As mentioned, this entails a worse performance in terms of accuracy in detecting Δ_R and then leak location [18]. Moreover, the larger A_{ve}, the larger the volume of the water supplied by the S-PPWM. This implies a larger volume, and then a larger P^d, to avoid air entrance into the pipe. These observations, added to the fact that valves are often equipped with an anti water-hammer mechanism, restrict noticeably the margins of choice of the CV.

3.2. The role of the S-PPWM size and arrangement

In this section attention is focused on the role of the volume of the S-PPWM, W^d. As mentioned, W^d is divided in two parts: the lower one occupied by water, $W^d_{w,0}$, and the upper one by compressed air, $W^d_{a,0}$ (the subscripts w and a refer quantities to water and air, respectively). On one side, the role of $W^d_{w,0}$ is clear: when the CV is open and the S-PPWM supplies the pipe, air entrance must be avoided. On the other side, the role of $W^d_{a,0}$ is not merely the one of a sort of air cushion transmitting pressure from the compressor to the below water. In fact, as shown in [26], it influences the stability, ϵ, of the generated pressure signal, defined as:

$$\epsilon = \frac{h^M_\theta - h^M_T}{h^M_0} = \frac{E}{h^M_0} \tag{3}$$

where E = total decay of the pressure signal during the observation time, T (Fig. 4). The value of T depends on the procedure followed within TTBTs. Precisely, if attention is focused on the identification of Δ_R, it is $T = \tau$ [15, 17]. It is worth noting that to minimize the decay of the pressure signal improves the performance of the procedure mainly in terms of leak sizing. In fact, the decay pattern does not impede the identification of the leak whereas it may cause an error on the measurement of Δ_R and then the evaluation of the leak size.

According to Eq. (3), the smaller ϵ, and then E, the more stable the pressure signal during T, the more accurate the evaluation of Δ_R. With regard to such a feature, it is important to note the relevance of a precise evaluation of Δ_R within leak detection surveys. In fact, the successive intervention may be decided or not depending on the size of the detected leak.

Numerical experiments executed in [26] indicate that ϵ is a function of three dimensionless quantities:

$$\epsilon = f_2(\upsilon, \zeta, \beta) \tag{4}$$

where $\upsilon = W^d_{a,0}/W^d$, $\zeta = A_{ve}/A$, and $\beta = h^d_0/h^p_0$. Precisely, ϵ increases with ζ and β, whereas it decreases with υ. The mentioned numerical experiments pointed out that $\upsilon = 0.20$ guarantees a viable stability of the pressure signal whereas values of ζ smaller than 0.13 ensure a good performance. On the contrary, a single reference value of β cannot be indicated since ϵ increases linearly with such a quantity.

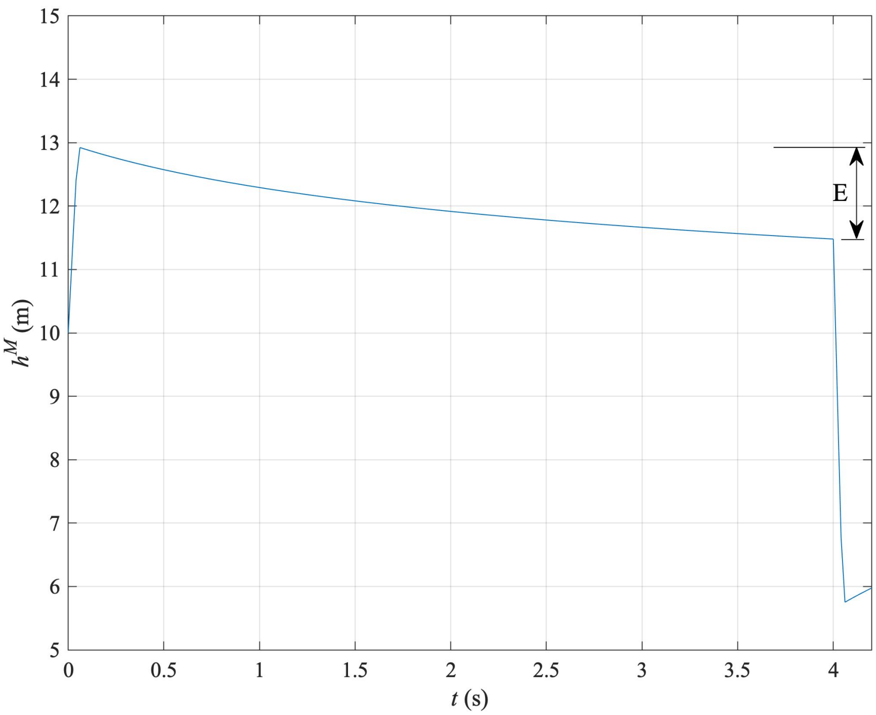

Figure 4: Pressure signal acquired at section M for a DN 600 single pipe, with $a = 1000$ m/s, $L = 2000$ m, $h_0^d = 15$ bar, $h_0^p = 1$ bar, $\upsilon = 0.20$, $A_{ve} = 1.5762{\cdot}10^{-4}$ m^2, and $\theta = 50$ ms.

4. Designing the S-PPWM: materials and methods

As discussed above, for a given CV, to design the S-PPWM, two quantities must be evaluated: the total volume, W^d, and maximum operating pressure, h^d_{max} $(= h^d_0)$. These values must be a good compromise between the performance – Δ (as large as possible) – and its portability (i.e., weight and size, as small as possible). Moreover, with the aim of limiting the cost of the device, the size of the S-PPWM must be selected among those in commercial catalogues.

The suitability of $W^d_{w,0}$ and $W^d_{a,0}$, and then the one of W^d, can be assessed by integrating numerically the equations governing the transient generated by the fast opening of the CV:

$$\frac{\partial h}{\partial x} + \frac{Q}{A^2 g}\frac{\partial Q}{\partial x} + \frac{1}{gA}\frac{\partial Q}{\partial t} + J = 0 \tag{5}$$

$$\frac{\partial h}{\partial t} + \frac{a^2}{gA}\frac{\partial Q}{\partial x} = 0 \tag{6}$$

being the momentum and continuity equation, respectively; in Eqs.(5) and (6), Q = discharge, and J = friction term. Such equations, integrated numerically within the Method of Characteristics (MOC), give rise to algebraic equations, in finite differences terms.

For the case of the single pipe of Fig.2, as an example, the related boundary conditions can be written as [9, 10]:

$$h^M_t = C^{-M}_t + B^M_t Q^M_t \tag{7}$$

$$Q^M_t = \frac{W^d_{a,t} - W^d_{a,t-\Delta t}}{\Delta t} \tag{8}$$

$$Q^M_t = A_{ve}\sqrt{2g\left(h^d_t - h^M_t\right)} \tag{9}$$

$$h^d_t (W^d_{a,t})^n = constant \tag{10}$$

at the S-PPWM – which are the compatibility equation along the negative characteristic line, the mass balance equation, the orifice equation, and the state equation for the air, respectively – and

$$q^l_t = A_{le}\sqrt{2g(h^l_t - z^l)} \tag{11}$$

the orifice equation at the leak, with A_{le} = leak effective area, and z^l = leak elevation (assumed as equal to 0 for the sake of simplicity), and

$$h^R = constant \tag{12}$$

at the constant level supply reservoir. In Eqs.(7)-(12), C^- is a constant defined in the MOC along the negative characteristic line depending on the hydraulic resistance, pressure head and discharge at the downstream computational node (i.e., node M in Fig. 2) at the previous instant of time, $B = a/gA$, and $n = 1.41$ under the usual hypothesis of adiabatic thermodynamic transformation of the air; the subscripts t, Δt, and M indicate the time elapsed since the beginning of the transient (i.e., when the CV valve opens), the time step, and the pipe section M immediately downstream of the CV. As mentioned, if, as usual, the measurement section is located immediately downstream of the CV, it is $h_t^M = h_t^p$.

Once integrated the governing equations, the total volume of the water supplied by the S-PPWM, $W_{w,tot}^d$, can be evaluated by means of the following relationship:

$$W_{w,tot}^d = \sum_{i=1}^{m} Q_i^M \Delta t = W_{w,0}^d - W_{w,T}^d \tag{13}$$

with $m = T/\Delta t$. The assumption $T = \tau$ ensures that even a leak located very close to the supply reservoir can be detected with the S-PPWM still partially full of water. The effectiveness of the S-PPWM in terms of supplying water, with no air entry during the transient tests, is assured if it is $W_{w,0}^d > W_{w,tot}^d$.

In the below numerical simulations, a stainless steel vessel will be considered since nowadays such a material is the most used for devices in drinkable water pipe systems. However, no restriction to the proposed design procedure derives from such an assumption. According to the commercial stainless steel vessels and experiments carried out both in the laboratory and in real systems, it is assumed W^d = 100 L, to which corresponds P^d = 40 kg, and h_{max}^d = 15 bar. It is worth noting that in the Italian legislation, such a value of h_{max}^d is the mentioned critical pressure value, h_{crit}.
With regard to the choice of the CV, the extensive experimental activity executed at the Water Engineering Laboratory (WEL) and in several real TMs indicates the pneumatic valve Prisma - Paw 3/4" ($A_{ve} = 1.5762 \cdot 10^{-4}$ m^2) as a reliable device. In fact, the duration of the opening maneuver, θ, of this

valve is only 50 ms. It is important to point out that in most cases such a value of θ ensures the validity of Eq.(1).

5. S-PPWM performance assessment

In this section, the performance of the proposed S-PPWM is checked in a large range of TMs characteristics. Precisely, elastic (i.e., concrete and metallic) and polymeric (e.g., polyethylene) water pipes are considered. As a consequence, representative values of the pressure wave speed, a, are 1000 m/s [33, 34] and 400 m/s [35, 36], respectively. Regarding the size of the test pipe, the range of the explored nominal diameters, DN, is 400-1300 mm and 400-800 mm for elastic and polymeric pipes, respectively. According to the usual functioning conditions of real TMs, h_0^p changes in the range 1-10 bar. In fact, values of h_0^p smaller than 1 bar are usually excluded since they can give rise to back-flow phenomena through leaks whereas values larger than 10 bar are quite unusual. With regard to the values of $W_{w,0}^d$ and $W_{a,0}^d$, according to [26], to ensure the pressure signal stability, it is set $v = 0.20$. For the considered cases, the values of Δ, given by Eq. (1), are reported in Fig. 5a and 5b, for elastic and polymeric pipes, respectively.

Fig. 5 plots show that in all the considered cases safe transients are generated, with 6 m being the maximum value of Δ (for $a = 1000$ m/s). Moreover, for given DN and h_0^p, in polymeric pipes the generated pressure wave is smaller than the one for elastic pipes because of the smaller value of a. Irrespective of pipe material, the smaller DN and h_0^p, the larger Δ. On the other hand, with increasing DN and h_0^p, especially for polymeric pipes, Δ decreases to values smaller than 1 m. However, as shown in [18, 25], such values may allow a reliable diagnosis of the test TM. As a consequence, in terms of the generated pressure wave, it can be affirmed that, for the given CV, $h_0^d = 15$ bar is a proper design value in a large range of TMs characteristics and functioning conditions. However, such a value of h_0^d can be reduced within a more deepened analysis of both the test pipe and equipment. To verify the adequacy of the chosen value of W^d, the total volume of the supplied water, $W_{w,tot}^d$ – given by Eq.(13) – has been evaluated by integrating numerically the transient governing equations, in the time interval $T = \tau$. In the executed numerical simulations, the pipe length, L, changes in the range 0.5-25 km, that is compatible with real TMs. Moreover, for the sake of safety, it is assumed $h_0^d = 15$ bar and $h_0^p = 1$ bar, corresponding to the most severe condition in terms of S-PPWM emptying. In fact, the larger the

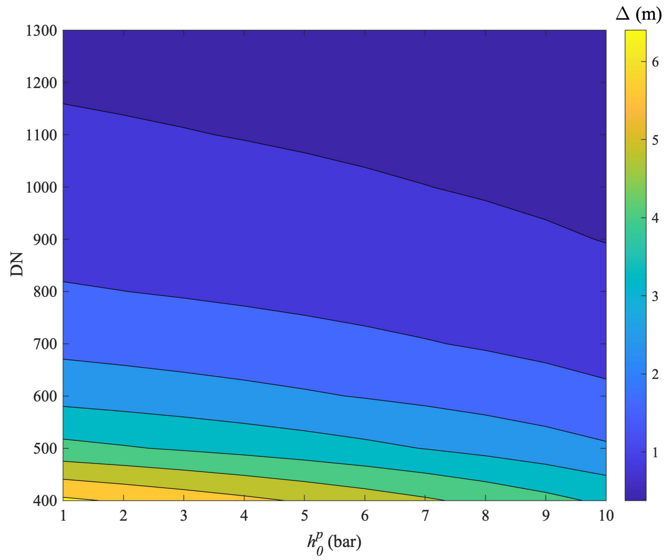

(a)

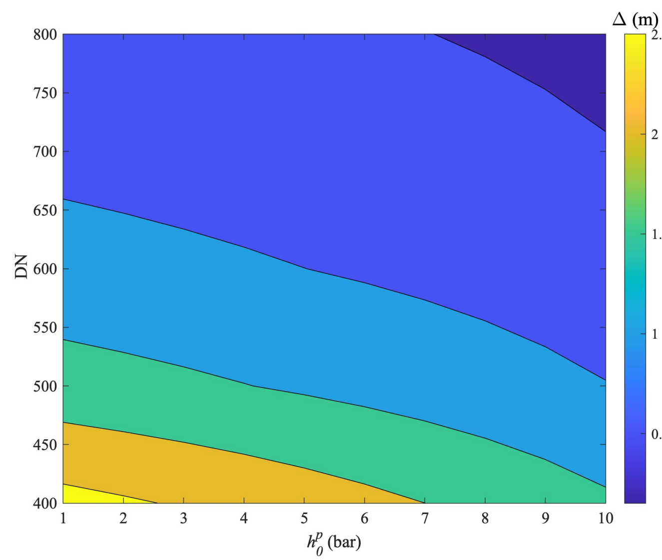

(b)

Figure 5: Values of the generated pressure wave, Δ, for $A_{ve} = 1.5762{\cdot}10^{-4}$ m^2, $h_0^d = 15$ bar, for different values of h_0^p and DN, and for: a) $a = 1000$ m/s (elastic pipes), and b) $a = 400$ m/s (polymeric pipes).

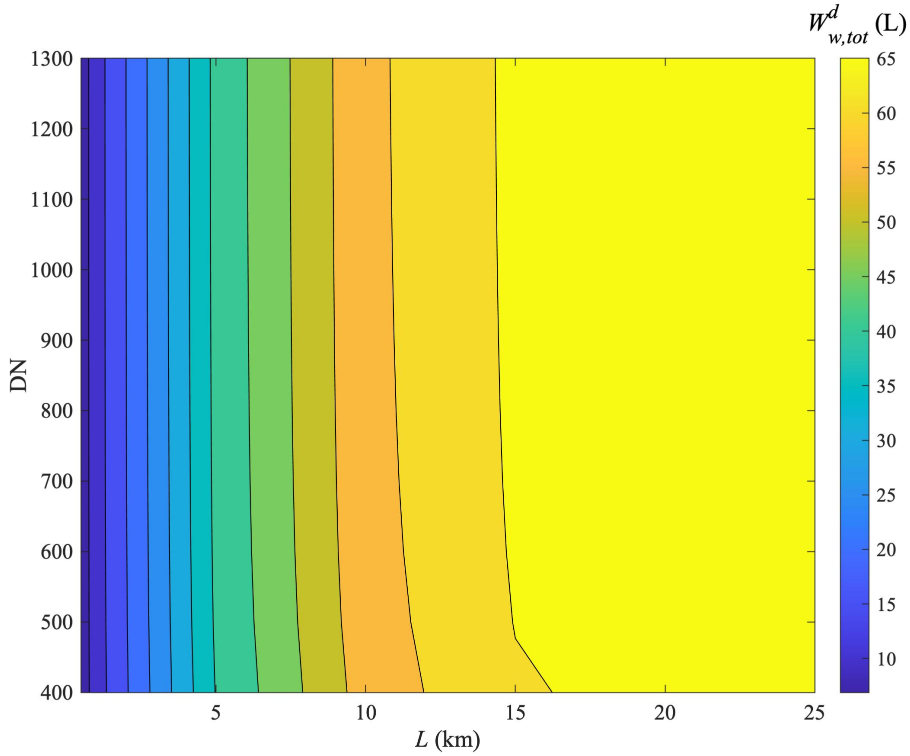

Figure 6: Total water volume, $W^d w, tot$, supplied by the S-PPWM during the observation time, $T = \tau = 2L/a$, vs. L and DN, for $a = 1000$ m/s (elastic pipes).

difference $h_0^d - h_0^p$, the larger $W^d_{w,tot}$. The results of the numerical simulations for elastic pipes ($a = 1000$ m/s) are shown in Fig. 6. In this figure, the contour lines are quite vertical meaning that the pipe diameter does not significantly affect $W^d_{w,tot}$, whereas L plays an important role. Precisely, as might be expected, the longer the pipe, the larger the volume of the water supplied by the S-PPWM during T, and then the higher the risk of the device emptying. Moreover, very important, Fig. 6 shows that, for all the considered conditions, the value of $W^d_{w,tot}$ is smaller than 80 L. This ensures that the S-PPWM does not empty and then no air enters the pipe during the transient test.

Because of the shown negligible dependence of $W^d_{w,tot}$ on the pipe diameter, for polymeric pipes ($a = 400$ m/s), in Fig. 7 the values of $W^d_{w,tot}$ are reported for just a single value of DN (= 600 mm). As a reference, in this figure the corresponding curve for an elastic pipe, with the same DN, is also

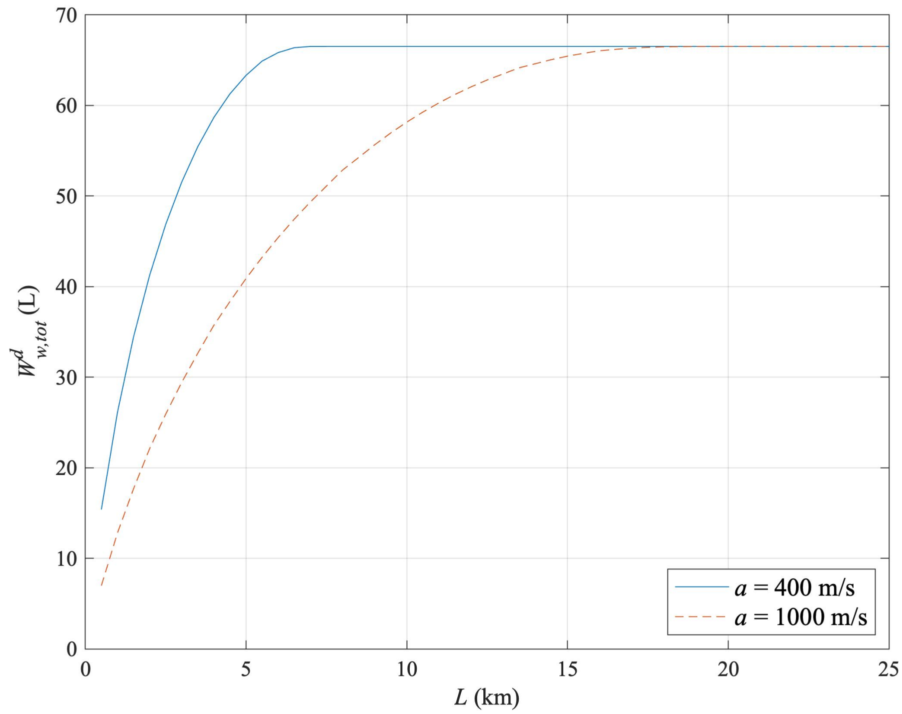

Figure 7: Total water volume, W^dw, tot, supplied by the S-PPWM during the observation time, $T = \tau = 2L/a$, vs. pipe length, L, for DN 600, a = 400 m/s (polymeric pipe) and a = 1000 m/s (elastic pipe).

depicted. It is noteworthy that both curves show an asymptotic behavior with its maximum value reached more rapidly for the polymeric pipe than for the elastic one. This is due to the fact that, because of the smaller value of a, in polymeric pipes the characteristic time lasts longer and then a larger amount of water is supplied by the S-PPWM.

6. Detecting leaks using the S-PPWM

Once the characteristics of the S-PPWM and transient test have been defined, the value of Δ_R can be evaluated by means of the following relationship [31]:

$$\Delta_R = \left(1 + 2\frac{A}{A_{le}^2}\frac{q_0^l}{a}\right)^{-1}\Delta \tag{14}$$

where q_0^l, the pre-transient discharge through the leak, is given by:

$$q_0^l = A_{le}\sqrt{2g(h_0^l - z^l)} \tag{15}$$

By combining Eqs. (1), (14), and (15), Δ_R has been determined for different values of q_0^l and test pipe characteristics. In the below analysis, as discussed above, it is considered $\Delta_R^M = 2\Delta_R$. As an example, varying DN (400-700 mm) and h_0^p (1-6 bar) and assuming $h_0^d = h_{max}^d = 15$ bar, $a = 1000$ m/s, and $A_{ve} = 1.5762{\cdot}10^{-4}$ m^2, the obtained values of Δ_R^M are shown in Fig. 8a, 8b, and 8c for $q_0^l = 1$ L/s, 2 L/s, and 5 L/s, respectively. With regard to such values of q_0^l, two comments are of interest. The first is that they must be considered as extremely small for a TM where much larger discharges are conveyed. The second comment is that they are smaller than the measurement error of the discharge flow-meters usually installed in large diameter TMs.

These figures show that, for $q_0^l = 1$ L/s, the maximum value of Δ_R^M is 0.25 m, whereas for $q_0^l = 5$ L/s it is equal to about 1.2 m. Moreover, for all the considered values of q_0^l, the minimum value of Δ_R^M drops to few centimeters when DN and/or h_0^p increase. This implies that the detectability of extremely small leaks in the pressure signal decreases for large diameters and pipe pressure. As a consequence, if the detection of very small leaks is crucial, a preliminary analysis is recommended to choose the proper data acquisition system, location of the measurement section, and pressure transducer. That said, it is evident that the analysis of the pre-transient pressure signal is crucial to assess whether a given Δ_R is readable. In the next section this key point is addressed in more detail.

7. Refinement of the transient test procedure

Once the S-PPWM has been designed, its performance can improve significantly if further arrangements are taken within a sort of second order design. In the below subsections, attention is focused on the stability of the pressure signal and entity of Δ, that are strongly linked.

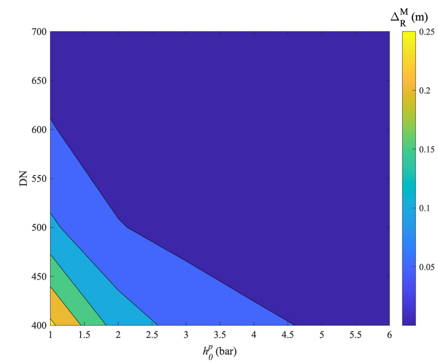

(a)

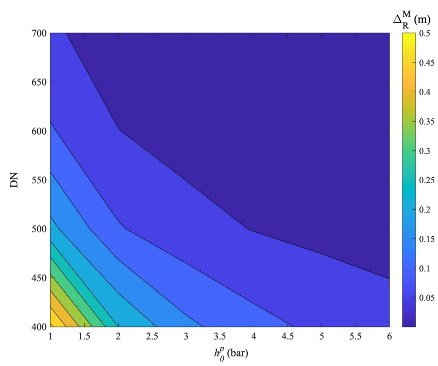

(b)

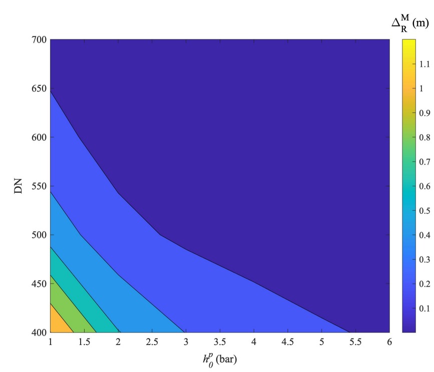

(c)

Figure 8: Values of the pressure wave measured at section M, Δ_R^M, for a = 1000 m/s, h_0^d = 15 bar, $A_{ve} = 1.5762 \cdot 10^{-4}$ m^2, different values of DN and h_0^p for: a) q_0^l = 1 L/s, b) q_0^l = 2 L/s, and c) q_0^l = 5 L/s.

7.1. *Maximizing the stability of the pressure signal*

As discussed above, setting h_0^d at 15 bar and reducing h_0^p, maximize Δ. On the other side, this implies large values of β $(=\frac{h_0^d}{h_0^p})$ and then a smaller stability of the pressure signal. Then, when planning a transient test, it is crucial to adjust the value of h_0^d and h_0^p in order to reduce ϵ as possible, but keeping Δ large enough for sizing even small leaks. In this context, it is important evaluating the minimum allowable value of Δ, as discussed in the next subsection. Another option is to increase the initial air volume, $W_{a,0}^d$, with respect to $W_{w,0}^d$. Such a refinement is viable only if the total supplied water, $W_{w,tot}^d$, is smaller than $W_{w,0}^d$. On the contrary, minimizing ϵ by means of a single CV with distinctive characteristics is not an easy action because of the mentioned poor marketplace of fast opening valves. A possible option, but to be checked before in the lab, is to to connect the S-PPWM and the test pipe by means of two valves in series .

7.2. *A criterion for evaluating the minimum detectable reflected pressure wave*

The quality of the measured signals is due to the characteristics of the used measurement equipment – e.g., probes, cables, and connections – and test pipe characteristics. With regard to the former feature, a preliminary in-field check is needed before the execution of the tests as the performance of the measurement equipment may deteriorate in time. With regard to the latter feature, the flow conditions in the TM, and the distance of the measurement section from singularities (e.g., curves) must be taken into account. However, since the evaluation of the performance of each single component/feature is quite difficult to execute in the field, a global approach could be followed. As an example, it could be based on the analysis of the pre-transient pressure signal, according to the encouraging results obtained at Water Engineering Laboratory where several tests have been executed in steady-state conditions on a high density polyethylene pipe (L = 188 m, DN 110) supplied by a reservoir. As an example, in Fig. 9, three pre-transient pressure signals acquired with an acquisition rate of 2048 Hz at section 1 (Fig. 10a) of the laboratory pipe are reported. The chosen duration of the pre-transient observation, T_{pt} (= 5 s), is merely illustrative and obviously larger values of T_{pt} can be adopted.

Plots on the left side of Fig.9 report the change of the pressure head with respect to the mean value Δh $(= h - \bar{h}$, with $\bar{h}$ being the mean value of $h)$.

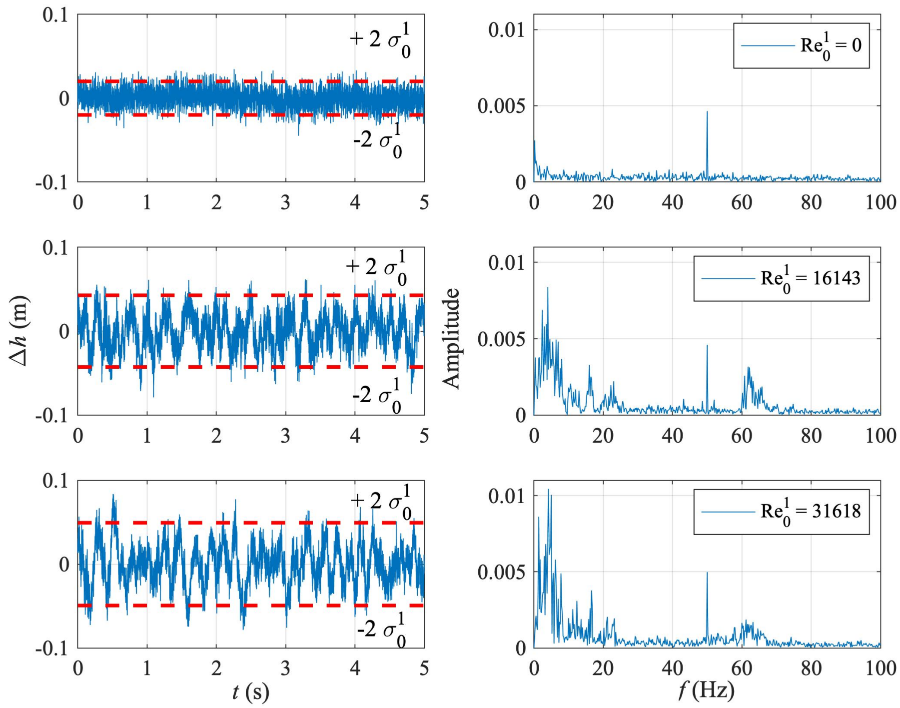

Figure 9: Change of the pressure head, Δh, with respect to the mean value (plots on the left), with indicated the relevant standard deviation, σ_0^1, and corresponding fast Fourier transforms (plots on the right) for different values of the pre-transient Reynolds number at the measurement section 1, Re_0^1, of the laboratory pipe at WEL (Fig.10a).

Plots on the right side show the corresponding fast Fourier transforms of Δh for a frequency, f, up to 100 Hz. As expected, for a given equipment, the larger Re_0^1 the larger Δh, with $Re_0^1(= Q_0 D/(A\nu))$ being the pre-transient Reynolds number at the measurement section 1, and ν = water kinematic viscosity. Such a behavior is confirmed by the fast Fourier transforms of Δh, reported in the plots at the right side of Fig. 9. Precisely, when Re_0^1 is equal to 0 (still water), the frequency content of the pressure signal is small, whereas it increases with Re_0^1. To quantify the entity of the changes of Δh with Re_0^i, the standard deviation, σ_0^i, of the Δh signals of Fig. 9 has been evaluated. Successively, a range $[-2\sigma_0^i; +2\sigma_0^i]$ has been traced in this figure by red dashed lines. Fig. 10b shows the behavior of σ_0^i vs. Re_0^i in different sections of the laboratory pipe (Fig.10a) by using a pressure transducer with a different full scale and distance from the data acquisition system (DAQ). Even if a detailed analysis of the quantities affecting σ_0^i is beyond the aims of this paper, it can be observed that, for a given Re_0^i, the curves of Fig. 10b differentiate according to the location of the measurement section, used pressure transducer, and length of the electric connections to DAQ.

On the basis of such results, a possible criterion for evaluating the minimum detectable reflected pressure wave is to assume $\Delta_{R,min}$ equal to a threshold value, σ_{th}, evaluated on the basis of the measured pre-transient pressure signal. As an example, it could be considered $\Delta_{R,min} = \sigma_{th} = 2\sigma_0^i$. In such a context, in a real TM preliminary measurements must be executed in the accessible pipe sections to choose the best location in terms of the pressure signal quality (i.e., the smaller σ_0^i the better).

8. Operative procedure for designing the S-PPWM

On the basis of the obtained results and discussion, the procedure for designing the S-PPWM can be delineated as shown in the flow-chart graph of Fig.11.

The first step of this procedure includes a preliminary survey of the TM accessible sections where the S-PPWM can be installed and pressure signal measured. Three are the results of this survey. The first is the identification of the pressure value representative of the pre-transient pressure regime, h_0^p. The second result is the evaluation of the threshold value, σ_{th} – as the minimum value of σ_0^i – and then the one of $\Delta_{R,min}$. The third result is the selection of the location of the measurement section.

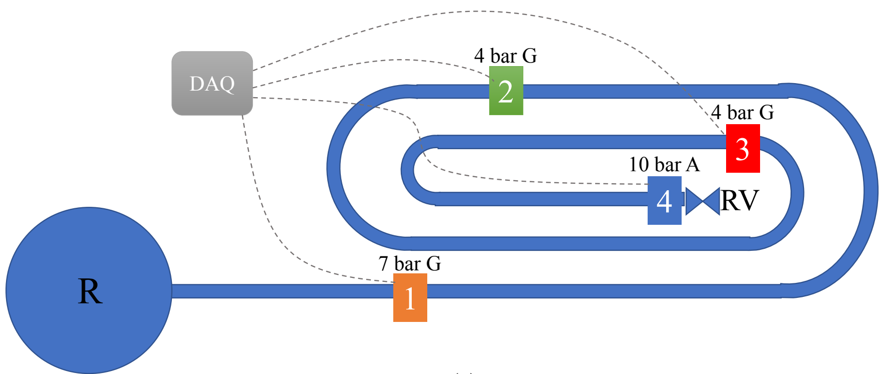

(a)

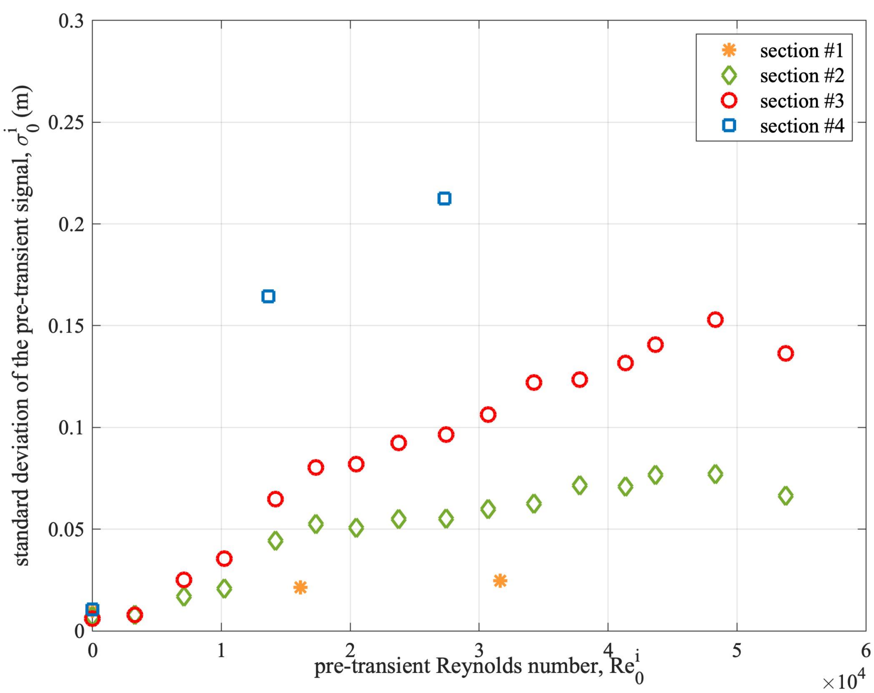

(b)

Figure 10: Experiments executed at the Water Engineering Laboratory (WEL) of the University of Perugia, Italy: a) laboratory pipe with indicated the location of the measurement sections, data acquisition system (DAQ), and full scale of the used pressure transducers, and b) standard deviation of the pre-transient pressure signal, σ_0^i, vs. pre-transient Reynolds number, Re_0^i.

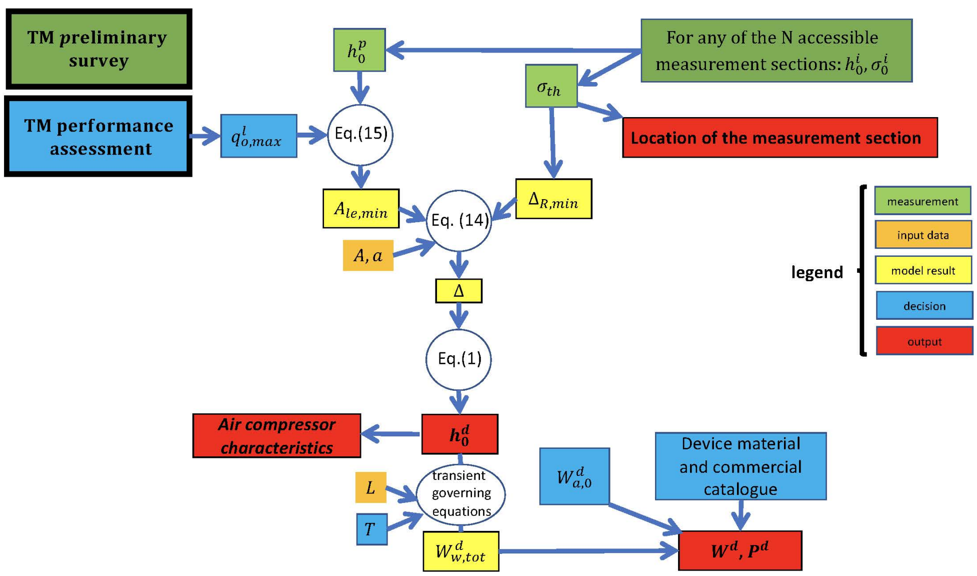

Figure 11: Operative procedure for the S-PPWM design.

Once fixed the value of the maximum admissible discharge that can be lost through the leak, $q^l_{0,max}$, the second step allows evaluating the minimum leak effective area, $A_{le,min}$, that can be detected, by means of Eq.(15). Successively, given $q^l_{0,max}$, $A_{le,min}$ and $\Delta_{R,min}$, as well as the test pipe cross-section, A, and pressure wave speed, a, the value of the pressure wave, Δ, that must be inserted is given by Eq. (14).

Within the third step, firstly the needed value of h^d_0 ($= h^d_{max}$) to generate Δ is evaluated by Eq. (1). On the basis of such a value of h^d_0, the proper air compressor can be identified. Successively, given the pipe length, L, and the chosen observation time, T, the total volume of the supplied water, $W^d_{w,tot}$, is obtained by integrating numerically the transient governing equations. In such a calculation, a first attempt value of the volume of the S-PPWM must be assumed. On the basis of the executed experiments, the value 100 L can be reliably considered.

In the fourth step, chosen the device material and according to the value of h^d_0 ($= h^d_{max}$), the corresponding list of commercial devices is selected. This will allow identifying, on the basis of the fixed value of the initial air volume, $W^d_{a,0}$, the total S-PPWM volume, W^d, and its relevant weight, P^d. Once evaluated W^d and P^d, a final decision can be taken about the suitability of the designed device in terms, as an example, of its portability. In case it were unsuitable, a different (larger) value of the the minimum detectable leak must be assumed. Of course, such a decision have implications on the quality of the survey and then performance of the stakeholder.

9. Conclusions

Nowadays, overarching principles for adequate water resources exploitation impose more attention to the condition of pressurised transmission mains (TMs), very important but aging infrastructures conveying water from the source to cities or large groups of users. This new approach somehow redeems the negligence of water managers in the past years and allows countering the deterioration of most TMs.

In this paper, criteria for the optimal and market-oriented design of the Smart-Portable Pressure Wave Maker (S-PPWM) for fault (leak) detection are presented. S-PPWM is an improved version of the PPWM device refined at the Water Engineering Laboratory (WEL) of the University of Perugia, Italy, and successfully tested both in laboratory [30, 18, 27, 28] and real [25] pipe systems. Such a device can be used within fault detection surveys of

TMs based on the execution of safe transient tests (the so-called Transient Test-Based Techniques - TTBTs).

The proposed design procedure addresses two crucial issues: i) to minimize the volume (and then improving the portability), and ii) to allow evaluating easily the minimum detectable leak, for a given test TM. Such a procedure takes into account not only the characteristics of the instrumentation device and possible measurement sections but also the functioning conditions of the test TM. In such a context, putting first the safety of the test pipe in terms of maximum generated overpressures, particular attention is also devoted to preventing air entry during transient tests to not affect the performance of the TM.

10. Acknowledgments

This research has been funded by the Hong Kong (HK) Research Grant Council Theme-Based Research Scheme and the HK University of Science and Technology (HKUST) under the project *Smart Urban Water Supply System (Smart UWSS)*. Support from Italian MUR and University of Perugia is acknowledged within the program *Dipartimenti di Eccellenza 2018-2022*. The support of Mr. Claudio Del Principe during laboratory experiments is highly appreciated.

[1] S. Hamilton, B. Charalambous, Leak detection: technology and implementation, IWA Publishing, 2020.

[2] K. Laven, J. Kler, Transmission mains in water loss control programs, in: Proc., ASCE Pipeline Conference, Seattle, Washington, United States, 2011, pp. 704–713.

[3] L. Laven, A. Lambert, What do we know about real losses on transmission mains?, in: Proc., IWA Specialised Conference Water Loss, 2012, pp. 1–10.

[4] Z. Liu, Y. Kleiner, State of the art review of inspection technologies for condition assessment of water pipes, Measurement 46 (1) (2013) 1–15.

[5] A. Cataldo, E. De Benedetto, G. Cannazza, N. Giaquinto, M. Savino, F. Adamo, Leak detection through microwave reflectometry: from laboratory to practical implementation, Measurement 47 (2014) 963–970.

[6] A. Cataldo, E. De Benedetto, G. Cannazza, a. Masciullo, N. Giaquinto, G. M. D'Aucelli, N. Costantino, A. De Leo, M. Miraglia, Recent advances in the tdr-based leak detection system for pipeline inspection, Measurement 98 (2017) 347–354.

[7] D. Kumar, D. Tu, N. Zhu, R. Ali Shah, D. Hou, H. Zhang, The free-swimming device leakage detection in plastic water-filled through tuning the wavelet transform to the underwater acoustic signals, Water 9 (10) (2017) 731.

[8] W. Wang, D. Yang, J. Zhang, L. Lao, Y. Yin, X. Zhu, A dead reckoning localization method for in-pipe detector of water supply pipeline: An application to leak localization, Measurement 171 (2021) 108835.

[9] E. B. Wylie, V. L. Streeter, L. Suo, Fluid transients in systems, Prentice Hall Englewood Cliffs, NJ, 1993.

[10] J. Swaffield, A. Boldy, Pressure surge in pipe and duct systems, Avebury Technical, England, 1993.

[11] B. Brunone, A transient test-based technique for leak detection in outfall pipes, J. of Water Resources Planning and Management 125 (5) (1999) 302–306.

[12] C. Capponi, S. Meniconi, P. J. Lee, B. Brunone, M. Cifrodelli, Time-domain analysis of laboratory experiments on the transient pressure damping in a leaky polymeric pipe, Water Resources Management 34 (2) (2020) 501–514.

[13] A. Colombo, P. Lee, B. Karney, A selective literature review of transient-based leak detection methods, J. of Hydro-Environment Research 2 (4) (2009) 212–227.

[14] S. Datta, S. Sarkar, A review of different pipeline fault detection methods, J. of Loss Prevention in the Process Industries 41 (2016) 97–106.

[15] X. Xu, B. Karney, An overview of transient fault detection techniques, in: Modeling and Monitoring of Pipelines and Networks, C. Verde and L. Torres (eds.), 2017, pp. 13–37.

[16] A. Ayati, A. Haghighi, P. Lee, Statistical review of major standpoints in hydraulic transient-based leak detection, J. of Hydraulic Structures 5 (1) (2019) 1–26.

[17] H. Duan, B. Pan, M. Wang, L. Chen, F. Zheng, Y. Zhang, State-of-the-art review on the transient flow modeling and utilization for urban water supply system (uwss) management, J. of Water Supply: Research and Technology - AQUA 69 (8) (2020) 858–893.

[18] S. Meniconi, B. Brunone, M. Ferrante, C. Massari, Small amplitude sharp pressure waves to diagnose pipe systems, Water Resources Management 25 (1) (2011) 79–96.

[19] M. Stephens, M. Lambert, A. Simpson, J. Vitkovsky, Calibrating the water-hammer response of a field pipe network by using a mechanical damping model, J. of Hydraulic Engineering 137 (10) (2011) 1225–1237.

[20] M. Taghvaei, S. Beck, J. Boxall, Leak detection in pipes using induced water hammer pulses, Int. J. of COMADEM 13 (1) (2010) 19–25.

[21] J. Shucksmith, J. Boxall, W. Staszewski, A. Seth, S. Beck, Onsite leak location in a pipe network by cepstrum analysis of pressure transients, J. of American Water Works Association 104 (8) (2012) E457–E465.

[22] S. H. Wang, T. T. Tsung, L. L. Han, Hydraulic square-wave pressure generator with a specific rotating valve, Measurement 42 (2009) 672–677.

[23] S. H. Wang, T. T. Tsung, L. L. Han, Method of generating a hydraulic step wave with a short rise time, Measurement 43 (2010) 935–940.

[24] J. Gong, M. F. Lambert, S. T. N. Nguyen, A. C. Zecchin, A. R. Simpson, Detecting thinner walled pipe sections using a spark transient pressure wave generator, J. of Hydraulic Engineering 144 (2) (2017) 0601702.

[25] S. Meniconi, C. Capponi, M. Frisinghelli, B. Brunone, Leak detection in a real transmission main through transient tests: deeds and misdeeds, Water Resources Research 57 (3) (2021) e2020WR027838.

[26] B. Brunone, M. Ferrante, S. Meniconi, Portable pressure wave-maker for leak detection and pipe system characterization, J. American Water Works Association 100 (4) (2008) 108–116.

[27] M. Ferrante, B. Brunone, S. Meniconi, Leak detection in branched pipe systems coupling wavelet analysis and a Lagrangian model, J. of Water Supply: Research and Technology - AQUA 58 (2) (2009) 95–106.

[28] D. Do, J. Lee, J. Kim, S. Kim, Study of leak detection in a pipeline system using a portable pressure wave generator, J. of Korean Society of Water and Wastewater 34 (2) (2020) 139–147.

[29] S. Meniconi, B. Brunone, M. Ferrante, In-line pipe device checking by short period analysis of transient tests, J. of Hydraulic Engineering 137 (7) (2011) 713–722.

[30] B. Brunone, M. Ferrante, S. Meniconi, Portable pressure wave-maker for leak detection and pipe system characterization, J. of American Water Works Association 100 (4) (2008) 108–116.

[31] C. Liou, Pipeline leak detection by impulse response extraction, J. of Fluids Engineering 120 (4) (1998) 833–838.

[32] M. Ferrante, B. Brunone, S. Meniconi, B. Karney, C. Massari, Leak size, detectability and test conditions in pressurized pipe systems, Water Resources Management 28 (13) (2014) 4583–4598.

[33] A. R. Halliwell, Velocity of a water-hammer wave in an elastic pipe, J. of Hydraulics Division 89 (4) (1963) 1–21.

[34] M. Karami, A. Kabiri-Samani, M. Nazari-Sharabian, M. Karakouzian, Investigating the effects of transient flow in concrete-lined pressure tunnels, and developing a new analytical formula for pressure wave velocity, Tunnelling and Underground Space Technology 91 (2019) 102992.

[35] D. Covas, I. Stoianov, J. Mano, H. Ramos, N. Graham, C. Maksimovic, The dynamic effect of pipe-wall viscoelasticity in hydraulic transients. Part I - experimental analysis and creep characterization, J. of Hydraulic Research 42 (5) (2004) 517–532.

[36] A. Soares, D. Covas, L. Reis, Analysis of PVC pipe-wall viscoelasticity during water hammer, J. of Hydraulic Engineering 134 (9) (2008) 1389–1395.